Title

Probabilistic solar power forecasting: An economic and technical evaluation of an optimal market bidding strategy

Authors

Visser, LR

AlSkaif, TA

Khurram, A

et al.

Publication Date

2024-09-01

DOI

10.1016/j.apenergy.2024.123573

Probabilistic solar power forecasting: an economic and technical evaluation of an optimal market bidding strategy

Lennard Visser, Tarek AlSkaif, Adil Khurram, Jan Kleissl, and Wilfried van Sark

***Abstract*—Solar power forecasting models are typically developed and evaluated based on technical error metrics, disregarding their economic value. However, achieving higher technical accuracy in these models does not necessarily translate into increased economic value, as the latter depends on energy trading value and market penalties. This paper addresses this interaction as well as the economic value of probabilistic forecasting models. It introduces a multistage stochastic bidding algorithm that optimizes the participation of a photovoltaic (PV) power plant in the day-ahead and intraday markets, while considering penalties incurred in the balancing market. The proposed approach relies on input scenarios generated from probabilistic forecasting models. A comparison is made between this approach and a reference method that relies on single-value forecasts. The bidding approaches are evaluated in terms of their technical accuracy and economic value. The results demonstrate the effectiveness of the proposed bidding approach as it outperforms the reference market bidding strategy. Additionally, the study examines the relationship between the accuracy and value of solar PV forecasting models, revealing a non-linear correlation.**

***Index Terms*—Photovoltaic power; probabilistic forecasting; stochastic optimization; electricity markets**

I. Introduction

Supporting policies and rapidly decreasing costs triggered the exponential growth of solar photovoltaic (PV) systems since the turn of the century. By the end of 2022, over 1.1 TWp of PV capacity was installed [1], thus forming a substantial contribution to the power supply system in many countries across the globe. The increasing share of solar PV generation, and its variable and intermittent nature, affects the operation of the electricity system posing various technical challenges. These include power quality issues, such as voltage and frequency fluctuations, as well as challenges related to the balancing of supply and demand [2]. As the proliferation of PV is expected to continue in the coming decades, reaching up to 70 TWp by 2050 [3], these technical issues are foreseen to form a major hurdle for its successful integration. Hence, (additional) measures are needed to allow for cost-effective integration of vast amounts of solar PV in the electricity grid [4]. Reliable solar power forecasting models are widely identified as a key element to support the effective integration of large amounts of solar PV systems in the electricity grid [5]. Accurate forecasts can assist in the timely scheduling of the dispatch of alternative generators and batteries, and therewith ensuring grid stability, while reducing the need for balancing reserves. Amongst others, this would result in a reduced need for balancing capacity, thus limiting the cost of PV integration.

The interest in solar forecasting models increased significantly over the last decades [6]. In recent years attention shifted towards probabilistic models, which are preferred over single-value models as they provide information regarding the uncertainty of the forecast. The performance of solar forecasting models is mostly captured with technical error metrics, e.g. mean absolute error and root mean square error in case of single-value models or the brier score and continuous rank probability score (CRPS) for probabilistic models [7]. As a result, the economic value of solar forecasting is commonly ignored. A couple of exemptions are found in literature, which explored the economic value of solar forecasting for standalone PV-systems in various ways [8]–[11]. These studies assessed the value of one or multiple solar forecasting models in the day-ahead market (DAM) in five regions in the United States [8], California [9], Spain [10] and the Netherlands [11], respectively. In addition, these studies explicitly compared the relation between technical and economic metrics. Yet, these studies only consider single-value forecasting models and ignore probabilistic models. Bracalae et al. [12] evaluates the economic value of two Bayesian-based probabilistic forecasting models, using cost-based indices. The metric therefore allows to express the economic performance of (probabilistic) forecasting models by normalizing the economic value over the maximum value per time interval, much similar to e.g. the weighted mean absolute error. However, since this study neglects the uncertainty in the defined bidding strategy, it ignores the potential of utilizing the additional value that is captured in probabilistic forecasts.

Besides, these studies [8]–[12] exclude the intraday market (IM), which can be used to correct for prediction errors that originate in DAM trading. As a result, studies that exclude the IM overestimate the imbalance caused by trading electricity from PV systems and underestimate the value of solar forecasting [13]–[15]. Silva et al. [14] identified the need for adequate strategies that can deal with a multi-settlement

L. Visser and W. van Sark are with the Copernicus Institute of Sustainable Development, Utrecht University, The Netherlands, email: l.r.visser@uu.nl; w.g.j.h.m.van.sark@uu.nl. T. AlSkaif is with the Information Technology Group, Wageningen University, The Netherlands, e-mail: tarek.alskaif@wur.nl. A. Khurram and J. Kleissl are with the Center for Energy Research and Department of Mechanical and Aerospace Engineering, University of California, San Diego, CA, email: akhhurram@ucsd.edu; jkleissl@ucsd.edu.

The authors would like to acknowledge the Hofvijverkring for their support through a fellowship grant. This work is part of the Energy Intranets (NEAT: ESI-BiDa 647.003.002) project, which is funded by the Dutch Research Council NWO in the framework of the Energy Systems Integration & Big Data programme.

framework (i.e. DAM and IM), while considering uncertainties to facilitate the successful integration of variable renewable energy sources in electricity markets and power systems. Various studies propose a wide variety of bidding strategies for wind power or wind and storage; an extensive overview is included in [16]. In contrast, only few studies consider the development of market bidding strategies for PV systems. While a variety of deterministic and stochastic market bidding strategies that consider a PV-battery system are proposed and applied to the DAM [17]–[19] or DAM and IM [20], [21], none of these studies considers a solar forecasting model. Few other studies include a solar forecasting algorithm in their proposed bidding strategy. For example, a bidding strategy for the DAM that considers stochastic optimisation using an analog ensemble model to predict the PV generation is proposed in [22]. The study compares the results for a PV-battery system to a standalone PV system. Similarly, David et al. [23] compare several single-value solar forecasting models when used to optimize the DAM trading of a PV-battery system in Australia. Silva et al. [14] proposed a multistage stochastic optimization model for the optimal bidding of a virtual power plant composed of a wind plant, solar PV plant, and battery. The model considers the DAM and IM and relies on an artificial neural network to generate a set of scenarios.

Overall, the current literature lacks studies that propose and evaluate stochastic bidding strategies for electricity markets that consider standalone PV systems and rely on solar forecasting models. Additionally, these studies do not address the value of integrating IM trading alongside DAM trading, nor do they utilize state-of-the-art probabilistic solar forecasting models. This paper aims to address these gaps by introducing a novel multistage stochastic optimization approach that generates a bid for market participants operating a PV system. The economic value of two probabilistic solar power forecasting models is evaluated, along with an examination of the relationship between the economic value and technical accuracy. The bidding strategy employs a multistage scenario-based stochastic optimization method, comprising a day-ahead (DA) and intraday (ID) unit, while considering the economic consequences of potential forecast errors. The latter is reflected by the imbalance penalty that is raised in the balancing market, where various imbalance scenarios are tested and compared. Uncertainty in the stochastic model is described through scenario creation using a statistical method that transforms time-independent probabilistic solar forecasts into interdependent scenarios. The proposed bidding strategy is compared to a reference bidding strategy that relies on various single-value and benchmark forecasting models. Hence, this paper quantifies the added value of probabilistic solar power forecasting over single-value forecasting, considering the IM in addition to DAM and demonstrates the effectiveness of handling different imbalance scenarios. Although the approach is demonstrated in a case study focused on market participation with a solar PV plant, it can be easily adapted for optimizing market participation with other assets such as wind plants, storage, and demand.

The remainder of this paper is organized as follows. Section II discusses the methods and error metrics. Section III describes the data. Section IV presents the results. The findings in this study are concluded in Section VI.

II. Methods

A. Stochastic bidding approach

This study presents a novel multistage stochastic bidding approach designed to optimize bidding strategies in electricity spot markets for a PV system, considering its inherent uncertainty of power generation. The bidding approach first aims to maximize the expected value of participating in the DAM by placing an optimized bid ($\dot{p}_{\text{DA}}$) for K forecast horizons, considering a set of Ω scenarios. The bid is generated by solving problem (1), as:

$$\underset{\dot{p}_{\text{DA}}}{\text{maximize}} \quad \sum_{\omega=1}^{\Omega}\sum_{t=1}^{K}\Big(\lambda_t \dot{p}_{\text{DA},t} + b_t\lambda^{+}(p_{\omega,t} - \dot{p}_{\text{DA},t}) - (1-b_t)\lambda^{-}(\dot{p}_{\text{DA},t} - p_{\omega,t})\Big) \tag{1a}$$

$$\text{subject to} \quad 0 \le \dot{p}_{\text{DA}} \le p_{\text{max}}, \tag{1b}$$

where $\lambda^{+/-}$ present the imbalance price as defined in Section II-E and b_t is a binary variable expressed as:

$$b_t = \begin{cases} 0, & \text{if } \dot{p}_{\text{DA},t} > p_{\omega,t} \\ 1, & \text{otherwise.} \end{cases} \tag{2}$$

The bid considers a set of scenarios, as well as the potential economic consequences of a foreseen excess ($\dot{p}_{\text{DA,t}} < p_{\omega,t}$) or shortage ($\dot{p}_{\text{DA,t}} > p_{\omega,t}$) of power delivered to the grid in real-time. In addition, electricity can only be exported and the market bid is restricted by the grid capacity that is assumed to be equal to the nominal installed PV capacity (p_{max}). Note that problem (1) results in a market bid expressed in power, whereas volume (energy) bids are placed in the market. Hence, the power bid is converted considering the temporal resolution (Δt), this also holds for the following problems.

Next, corrections to the initial DAM bid can be made in the IM, relying on updated PV power forecasts. The objective of this optimization problem is to maximize the expected value by bidding in the IM ($\dot{p}_{\text{ID}}$) considering the updated forecasts as well as the initial bid to the DAM. Again, the consequences of deviations in real-time are considered by the imbalance prices for up- and down-regulation. An optimal ID bid is retrieved by solving problem (3), as:

$$\underset{\dot{p}_{\text{ID}}}{\text{maximize}} \quad \sum_{\omega=1}^{\Omega}\sum_{t=1}^{K}\Big(\lambda_{\text{ID},t} \dot{p}_{\text{ID},t} + b_t\lambda^{+}(p_{\omega,t} - \dot{p}_{\text{bid},t}) - (1-b_t)\lambda^{-}(\dot{p}_{\text{bid},t} - p_{\omega,t})\Big) \tag{3a}$$

$$\text{subject to} \quad \dot{p}_{\text{bid}} = \dot{p}_{\text{DA}} + \dot{p}_{\text{ID}}, \tag{3b}$$

$$0 \le \dot{p}_{\text{bid}} \le p_{\text{max}}. \tag{3c}$$

B. Reference bidding approach

In the reference bidding approach market bids are based on single-value solar power forecasts. Since these single-value forecasts do not provide any information regarding the

uncertainty of the prediction, the potential monetary impact of an imbalance is not considered. Therefore, the DA reference bidding approach can be viewed as a simplified version of (1a), where the bid is generated by solving problem (4), as:

$$\underset{\dot{p}_{\text{DA}}}{\text{maximize}} \quad \sum_{t=1}^{K}\Big(\lambda_{\text{DA},t}\dot{p}_{\text{DA},t}\Big) \tag{4a}$$

$$\text{subject to} \quad \dot{p}_{\text{DA},t} = \hat{p}_t - p_{\text{curt},t}, \tag{4b}$$

$$0 \leq \dot{p}_{\text{DA},t} \leq \hat{p}_t, \tag{4c}$$

where p_{curt} is the curtailed power. In contrast to (1), this variable is made explicit in condition (4b) to prevent for bids that exceed the forecasted value while allowing for $\dot{p}_t = 0$. In practice, the reference bidding approach generates a bid that is equal to the single-value forecast except when negative market price occur. In the latter case, the market bid is set to 0.

Similarly, IM bids are generated by solving problem (5), as:

$$\underset{\dot{p}_{\text{ID}}}{\text{maximize}} \quad \sum_{t=1}^{K}\Big(\lambda_{\text{ID},t}\dot{p}_{\text{ID},t}\Big) \tag{5a}$$

$$\text{subject to} \quad \dot{p}_{\text{ID},t} = \hat{p}_t - \dot{p}_{\text{DA},t} - p_{\text{curt},t}, \tag{5b}$$

$$\dot{p}_{\text{bid}} = \dot{p}_{\text{DA}} + \dot{p}_{\text{ID}}, \tag{5c}$$

$$0 \leq \dot{p}_{\text{bid},t} \leq \hat{p}_t. \tag{5d}$$

C. Solar forecasting models

In this study, both single-point and probabilistic models are employed to forecast the PV power generation. The single-point forecasting models include a multi-variate linear regression (MLR), random forest regression (RF), PV and a smart (clear sky) persistence (SP) model. The probabilistic models considered are quantile regression (QR), quantile regression forest (QF) and clear sky persistence ensemble (CSPE). All forecasting models were previously introduced in [24] and are therefore not further discussed here.

Although the aforementioned models are used for both DA and ID forecasting, the input information they consider varies. The DA forecasting models consider the same predictor variables as discussed in [24]. These include various irradiance components, wind speed, temperature, cloud cover and pressure. In addition to these variables, the ID models also consider lagged PV generation values observed over the previous 3 hours.

In addition to being either single-value and probabilistic models, these models can be classified according to the input information they consider. The SP, MLR, RF, QR and QF receive new information at each forecast issue time. The CSPE model is only updated at midnight, whereas the PV model is updated following the issue of numerical weather predictions (NWPs) at midnight and noon.

D. Scenario generation

The interdependence structure of forecast errors on sequential time horizons is essential to support time-dependent decision making, like multi-market participation with a PV-battery system. Yet, probabilistic forecasts neglect this interdependence structure. Pinson et al. [25] proposed a statistical method that can successfully transform probabilistic forecasts to scenarios that consider the interdependence structure of the prediction errors. The method was originally developed for the purpose of wind power forecasting and was later also successfully adopted for net load forecasting, i.e. demand subtracted with solar generation [26]. In this study, the method is adopted for the purpose of building scenarios from probabilistic PV power forecasts. As a first step a random variable Y_k is generated from the probabilistic forecasts ($\hat{F}_{t+k|t}$), using the probability integral transform (PIT):

$$y_{k,t} = \hat{F}_{t+k|t}(p_{t+k}),\ \forall t \tag{6}$$

where $\hat{F}_{t+k|t}$ denotes the cumulative distribution function (CDF) of the probabilistic forecasts $\hat{f}_{t+k|k}$ and k is the forecast horizon. Given that the generated probabilistic forecasts are in a discrete form, it is necessary to convert them into a continuous CDF to facilitate the PIT. To achieve this, a smooth curve is fitted to the set of predicted quantiles.

A key assumption of the scenario generation method is for the probabilistic forecasts to be reliable, which implies that a sample from the predictive CDF should be statistically similar to the observations. This is true if Y_k is uniformly distributed on the unit interval, i.e. $Y_k \sim \text{U}[0,1]$.

Next, the probit function (Φ^{-1}) i.e. inverse of the Gaussian CDF can be applied to transform Y_k to a normally distributed random variable X_k with zero mean and unit standard deviation, i.e. $X_k \sim \text{N}(0,1)$:

$$x_{k,t} = \Phi^{-1}(y_{k,t}),\ \forall t. \tag{7}$$

Considering the transformed random variable X_k for each horizon k ($k = t_0, ..., K-1$), a random vector $\mathbf{X} = (X_1, ..., X_{K-1})^\intercal$ can be constructed. The assumption is made that $\mathbf{X}$ follows a multivariate Gaussian distribution, denoted as $\mathbf{X} \sim N(\mu_0, \mathbf{\Sigma})$, where μ_0 is a vector of zeros and Σ represents the covariance matrix capturing the temporal dependency between the forecast horizons of interest, $k = t_0, ..., K-1$. An unbiased estimation of the matrix $\mathbf{\Sigma}$ can be obtained by:

$$\mathbf{\Sigma_t} = \frac{1}{t-1}\sum_{j=1}^{t}\mathbf{X}_j\mathbf{X}_j^\intercal. \tag{8}$$

The temporal dependence captured in the covariance matrix is anticipated to change over time, and particularly in different seasons characterized by distinct prevailing weather patterns. The covariance matrix $\mathbf{\Sigma}$ that considers a subset of historical samples is therefore updated for each time-step. In an iterative process, the size of the subset was empirically set to 30 days.

By employing a multivariate Gaussian random number generator with parameters μ_0 and $\mathbf{\Sigma}$, a set of Ω scenarios is generated. These scenarios represent Ω realizations of the random vector $\mathbf{X}$. Subsequently, Ω realizations of $\mathbf{Y_k}$ can be constructed using the CDF (Φ):

$$y_{\omega,k} = \Phi(x_{\omega,k})\ \forall \omega, k. \tag{9}$$

As a last step, the forecast scenarios are generated with:

$$\hat{p}_{\omega,t+k|t} = \hat{F}^{-1}_{t+k|t}(y_{\omega,k}),\ \forall \omega, k. \tag{10}$$

Fig. 1 presents an example of the results for the presented scenario generation algorithm for a DA (Fig. 1a and b) and ID

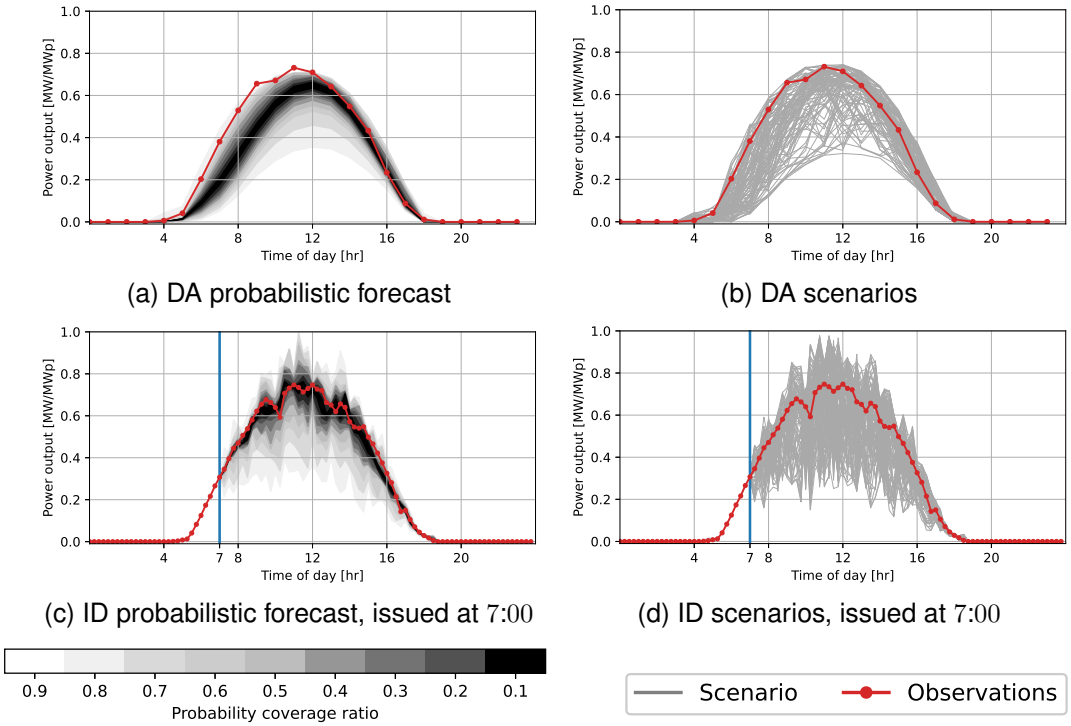

Fig. 1: Example of the DA (a,b) and ID (c,d) probabilistic forecasts and subsequent 100 scenarios of the expected PV power output for April 24, 2020. The blue vertical line in Fig. 1c and d presents the forecast issue time, i.e. 7:00.

forecast (Fig. 1c and d). Fig. 1a and c present the predictive distributions of the PV power output. The updated forecasts in Fig. 1c result in a sharper predictive distribution. This is especially observed in the first hours following the forecast issue time, which is exemplary for shorter forecast horizons. Note the different time resolution used in the models, where the maximum expected PV power output increases in case of the ID forecast as a result of reduced temporal smoothing.

E. Imbalance scenarios

Two different scenarios for imbalance penalization are considered. The first strategy assumes a static imbalance penalty:

$$\lambda^{+} = c_1 \tag{11}$$

$$\lambda^{-} = c_2, \tag{12}$$

where c_1 and c_2 present constants, which are varied as part of a sensitivity analysis to obtain the optimal value (See Section IV-E). In the second strategy the imbalance penalty depends on the electricity price and therefore varies over time. This dynamic imbalance penalty scenario is expressed as:

$$\lambda^{+} = \lambda_{\mathrm{DA},t} + c_1 \tag{13}$$

$$\lambda^{-} = \lambda_{\mathrm{DA},t} + c_2. \tag{14}$$

F. Operational aspects of bidding approach

The operational aspects of the bidding approach are defined by the market constraints and set the requirements to the solar forecasting models. Table I present a summary of the DAM and IM characteristics in the Netherlands, which define the lead-time, time horizon, temporal resolution and update rate.

TABLE I: Day-ahead and intraday spot market (DAM and IM) characteristics in the Netherlands.

	DAM	IM
Gate Closure Time	12:00 at D	Continuous
Lead-time	12 hr	5 min
Horizon	$12-36$ hrs	5 min to end of $D+1$
Resolution	Hourly	15 min
Update rate	Daily	Continuous
Type	Market clearing price	Pay-as-bid

G. Tools for evaluation

1) Solar forecasting models: The technical performance of the forecasting models are in this study primarily evaluated considering the continuous ranked probability score (CRPS). The CRPS is a numerical error metric that captures both the reliability and sharpness of probabilistic models. The CRPS can also be applied to assess the performance of single-point models, where the value is comparable to the mean absolute error [27]. The CRPS rewards a high concentration of the forecasted probability around the target value. The CRPS is expressed as:

$$CRPS = \frac{1}{T}\sum_{t=1}^{T}\int_{-\infty}^{\infty}(F_t(x) - \hat{F}_t(x))^2 dx, \tag{15}$$

where $F_t(x)$ and $\hat{F}_t(x)$ are the CDFs of the observations and forecasts at time-step t in T. In (15) $F_t(x)$ presents a cumulative-probability step function as it describes a single-value that jumps from 0 to 1 at the observed PV power generation [7]. Similarly, in case of a single-point forecast $F_t(x)$ presents a step function.

2) Solar scenarios: The PV power generation scenarios are evaluated in two steps. First, the calibration of the proba-

bilistic forecasting models and the assumption of a uniform distribution are assessed using a PIT histogram. A uniform distribution indicates that the forecast probabilities are well calibrated with the actual observations. The histograms are evaluated separately for each forecast horizon, considering consistency bars that present a lower and upper bound to account for randomness as suggested in [28].

Second, the scenarios are evaluated using two prerank functions: the average rank and band depth rank histogram (ARH and BDH), as set forth in [26] and originally proposed in [29]. These prerank functions provide insights in the calibration of scenarios and their interdependence structure. In particular, the ARH provides insights in the distribution of multivariate scenarios similarly to the PIT histogram does for univariate ensemble members, whereas the BDH assesses the correlation. The objective of a prerank function is to rank the trajectories of the generated scenarios and observation vector. The results can be visualized in a rank histogram, which quantifies the frequency of observations that fall between two ensemble members. The rank histogram is evaluated similar as a PIT histogram, where a uniform distribution of the rank histogram indicates well calibrated multivariate scenarios. To this end, the scenarios ($\mathbf{p}_\omega$) and observation vector ($\mathbf{p}$) are collected in a matrix B with dimensions $K \times J$, where $J = S + 1$. The rank histograms are then calculated following three main steps. First, univariate preranks are assigned to the ensemble members and observations with:

$$c_k(\mathbf{p}_\omega) = \sum_{j=1}^{J} \mathbf{1}\{p_{j,k} \leq p_{\omega,k}\}, k = 1, \ldots, K. \tag{16}$$

where $\mathbf{1}$ denotes an indicator function and c_k presents the prerank for each k-ensemble member or observation. As a second step, the multivariate preranks can be calculated and assigned to the scenarios and observation vector using the prerank functions π_B^{ARH} and π_B^{BDH}, respectively:

$$\pi_B^{ARH}(\mathbf{p}_\omega) = \frac{1}{K} \sum_{k=1}^{K} c_k(\mathbf{p}_\omega), \tag{17}$$

$$\pi_B^{BDH}(\mathbf{p}_\omega) = \frac{1}{K} \sum_{k=1}^{K} (J - c_k(\mathbf{p}_\omega))(c_k(\mathbf{p}_\omega) - 1). \tag{18}$$

As a third step, the rank histogram bin (b) of the observation vector is found per prerank function within the collection of preranks presented in B with:

$$b = 1 + \sum_{s=1}^{S} \mathbf{1}\{\pi(\mathbf{p}_s) < \pi(\mathbf{p})\}. \tag{19}$$

The reader is referred to [29] for a complete discussion on the interpretation of the rank histograms.

3) Market participation: The economic performance of the forecasting models is measured considering the economic revenue (ER), which is calculated as:

$$ER = \lambda \dot{p}_{\text{bid}} + \begin{cases} \lambda^+(p - \dot{p}_{\text{bid}}) \text{ if } y > \dot{p}_{\text{bid}} \\ \lambda^-(p - \dot{p}_{\text{bid}}) \text{ if } y \leq \dot{p}_{\text{bid}} \end{cases} \tag{20}$$

where p is the PV power generation and $\dot{p}$ is the optimized bid to the electricity spot market. The value of λ^+ and λ^- are set by the transmission system operator (TSO) and depend on the state of the electricity system at time t. In practice surpluses are most often compensated, whereas deficits are penalized, but exemptions occur. Since for most of the time λ exceeds λ^+, trading energy in the spot markets is most profitable. Similarly, as λ^- is typically higher than λ, the costs of shortages exceed the initial profits made in the electricity spot markets.

III. Data collection

A. PV power generation

The PV power generation data is acquired by simulating the power output of a 1 MWp PV system, using a PV model from *pvlib* [30]. The steps required to simulate the PV power output are discussed in Section 2.2.1 of [24]. The model requires the input of the measured global horizontal irradiance (GHI), ambient and dew point temperature, wind speed and surface pressure, which are collected from the weather station in Cabauw, the Netherlands (51°97'N, 4°926'E) [31]. The measurements feature a 10 min resolution; 15 min and hourly values are obtained through resampling. In this study, data from 2018 to 2020 is considered.

B. Weather forecasts

Weather forecasts are for the same period obtained from the European Centre for Medium-Range Weather Forecasts (ECMWF) [32]. The weather forecasts are acquired from the 0:00 and 12:00 UTC model runs generated by the high resolution forecast configuration (HRES) of the Integrated Forecast System (IFS), which is a NWP system. As the forecasts feature a spatial resolution of approximately 9 km, specific values are obtained using spatial interpolation [32]. The collected variables include the ambient and dew point temperature, GHI, total cloud cover, zonal and meridonal wind speed and total precipitation. Additional predictor variables are created following the three post-processing steps discussed in [24]. As the forecasts are published with an hourly resolution, 15 min values are obtained by means of linear interpolation for all variables except GHI. The 15 min GHI values are found through linear interpolation of the clear sky index.

C. Electricity prices

Electricity spot market prices are collected from the ENTSO-E transparency platform [33]. As only DAM prices are publicly available, IM prices are assumed to be identical. This assumption is substantiated as average IM prices are very similar to and strongly correlate with DAM prices [34]. Yet, actual IM prices can still differ from DAM prices, possibly altering the results. This impact is however expected to be negligible as it will likely have a similar effect on all models. Furthermore, imbalance prices are acquired from TenneT, the TSO in the Netherlands [35].

IV. Results

A. Scenario generation

The scenario generation approach followed in this study (see Section II-D) assumes the probabilistic forecasts to be

TABLE II: Summary statistics of the transformed random variables X_k. The statistics present the mean (μ), standard deviation (σ), skewness (γ) and excess kurtosis (κ), expressed by the mean and standard deviation over all forecast horizons.

Model	$\bar{\mu}_X \pm \sigma(\mu_X)$	$\bar{\sigma}_X \pm \sigma(\sigma_X)$	$\bar{\gamma}_X \pm \sigma(\gamma_X)$	$\bar{\kappa}_X \pm \sigma(\kappa_X)$
QR	-0.016 ± 0.03	0.96 ± 0.02	-0.035 ± 0.05	-0.21 ± 0.14
QF	0.020 ± 0.02	0.94 ± 0.01	-0.044 ± 0.04	-0.22 ± 0.01

uniformly distributed $U[0,1]$ in order to transform the predictions to a normal distribution $N(0,1)$. Fig. 2 shows the validity of the assumption by presenting the PIT diagrams of the QR model. Although some outliers are found in the columns on the left, overall the results show that the assumption holds as most bars remain within the margins of the consistency bars presented by the dotted blue lines. The PIT diagrams in Fig. 2b, c and d indicate a general trend where the quantiles around the median are slightly under-represented, such that the surrounding quantiles are over-represented. This trend was also observed for forecast horizons that exceed 1 hr. Similar results were found for the QF model.

The right column in Fig. 2 presents the histogram of the random variable X_k for the same forecast horizons. Additionally, similar to Table 1 in [25] and Table 2 in [26], Table II summarizes the statistical characteristics of the distribution of X for both the QR and QF model, for all forecast horizons. The table shows the mean ($\bar{.}$) and standard deviation ($\sigma(.)$) of the mean (μ), standard deviation (μ), skewness (γ) and excess kurtosis (κ). The results obtained for the first four moments are similar to the results found in [25], [26]. Remarkable, however, is that in contrast to these studies, the results show a negative excess kurtosis implying that the distribution of X is flatter featuring slightly shorter tails compared to a standard normal distribution $N(0,1)$, i.e. less outliers are observed. Although the excess kurtosis values are low, this indicates that the predicted distributions could be sharper, which is in line with the results observed in the PIT-diagram visualized on the left side in Fig. 2. Overall, considering the first four moments, the distribution of X over all $\mathcal{K}$ is on average approximately similar to a standard normal distribution of $N(0,1)$.

Fig. 3 shows the ARH and BDH results for a single forecast issue time at noon for the next day (DA forecast) of the QR model. As the histograms show a flat distribution, the obtained results are considered satisfactory. Similar results are found for the other forecast issue times as well as the QF model.

B. DA and ID forecasts

The numerical technical results of the PV power forecasting models are summarized in Table III. The values present average values over all forecast horizons $\mathcal{K}$. For the ID and DA forecasts these concern 0-24 hr and 12-36 hr ahead, respectively. Note that the DA and ID forecast models cannot be compared directly, as the DA models consider an hourly resolution, where the ID models feature a quarterly resolution. In addition, for the probabilistic models, Table III presents the obtained CRPS values considering the probabilistic forecasts as well as the scenarios. In the latter, the CRPS is calculated by considering the scenarios as an equally spaced probabilistic forecast, i.e. considering Ω is 100 scenarios each scenario is assumed to present a 1% quantile. A few general conclusions can be drawn considering the DA and ID forecasts. First, Table III clearly shows that the probabilistic forecasting models outperform the single-value models. Second, the results demonstrate the dominance of the tree-based models, where the RF and QF models outperform all other DA and ID single-value and probabilistic models, respectively. Yet, these differences in the CRPS are much more significant for DA forecasts compared to ID forecasts. Furthermore, the accuracy obtained for the generated scenarios are similar to the probabilistic models from which they originate.

TABLE III: The CRPS per DA and ID PV power forecast model over all realizations of $\mathcal{K}$ forecast horizons.

Model	DA		ID	
	original	scenario	original	scenario
SP	11.1		11.0	
PV	9.3		8.6	
MLR	8.3		7.3	
RF	6.8		7.1	
CSPE	7.9		7.9	
QR	6.0	6.0	5.2	5.2
QF	**4.6**	**4.7**	**4.8**	**4.8**

Fig. 4 shows the CRPS of the ID forecasting models per forecast horizon. As expected the accuracy of the models is highly affected by the forecast horizon. In general, the results in Fig. 4 indicate that the CRPS deteriorates with an increasing horizon, especially within the first hour. In short, this is explained by the temporal correlation of the PV power output. The lagged generation values form the most important predictor variables for predictions that feature a forecast horizon of up to 1 hr ahead. Model simulations show that as the forecast horizon increases, the NWP variables gain importance and these predictor variables surpass the importance of the lagged values from forecast horizons that exceed 1 hr ahead. This observation is exemplified by the disconnection of the CRPS trajectory of the SP model compared to the other single-value models MLR and RF. The performance of the SP model deteriorates more rapidly and significantly compared to the MLR and RF models, as it only considers the PV power output that is available at the forecast issue time and excludes the NWP variables. Since the NWP variables are only updated twice per day, the accuracy of the ID forecasting models stabilizes from the point that these variables predominate. The latter also explains the more or less constant performance of the PV model. In case more NWP runs would be available, improved model accuracy's are expected especially for shorter forecast horizons.

Furthermore, Fig. 4 shows that tree-based models (RF and QF) dominate by outperforming other single-value and probabilistic models, respectively, for all forecast horizons.

C. Market trading

The technical and economic results of participation in spot markets are, for various forecast horizons, summarized in Table IV and depicted in Fig. 5. Since the results for $k > 3$ hrs ahead are very similar to $k = 3$, these are excluded from Table IV. Note that in case of IM trading, the DAM

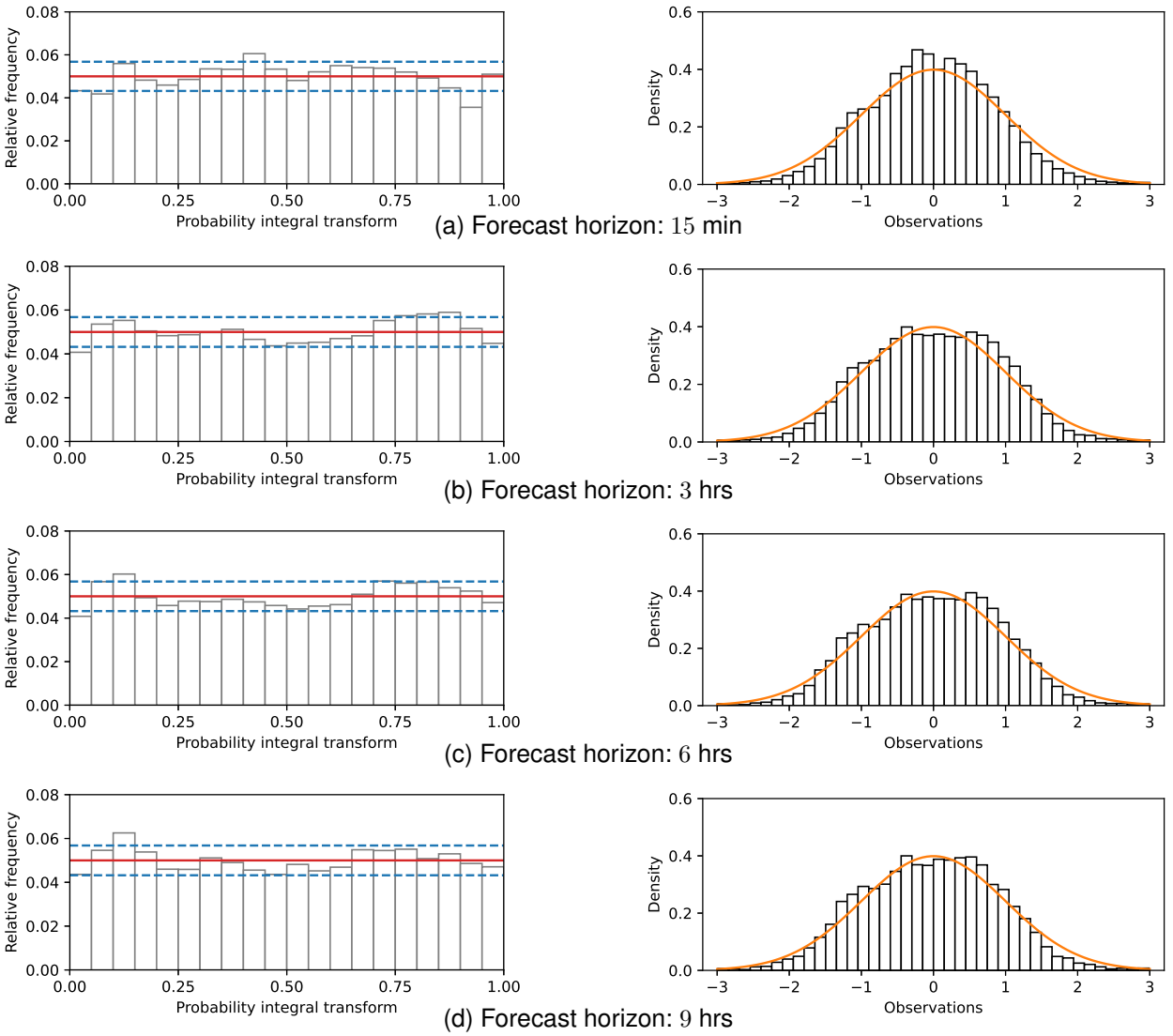

Fig. 2: The probability integral transform (Y_k) on the left and observed transformed random variable (X_k) on the right for four distinct forecast horizons of the QR model. The red line presents a perfectly calibrated forecast for U[0,1], the blue dotted lines indicate the consistency bars. The orange line presents the probability density function of a normal distribution N(0,1). Similar results are found for the QF model.

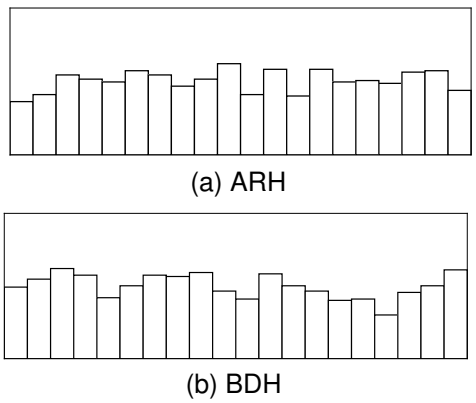

Fig. 3: Average rank histogram (ARH) and band depth histogram (BDH) for a single forecast issue time, i.e. 12:00 at D. Similar results are found for other forecast issue times.

trades are followed by IM trades considering the specified horizon. The results are compared to market participation in case of perfect solar forecasting, i.e. considering PV power measurements (red horizontal bar). The results in Table IV show an improved performance of market participation, in terms of the imbalance caused and revenues generated, when DAM trades are combined with IM trades. In general, the results show a trend in improved performance as the forecast horizon reduces with higher marginal gains related to IM trading. Hence, most value lays within the final moments prior to delivery and therefore last minute trading is preferred from a perspective of the PV plant operator. This observation holds for all models that receive updated information at each forecast issue (SP, MLR, RF, QR and QF). Furthermore, considering the best performing model per forecast horizon, revenues increase with 21.1% from 22.3 k€/MWp to 27.1 k€/MWp per year when DAM trades are updated with IM trades. As a result, the economic revenues are almost equal to the revenues

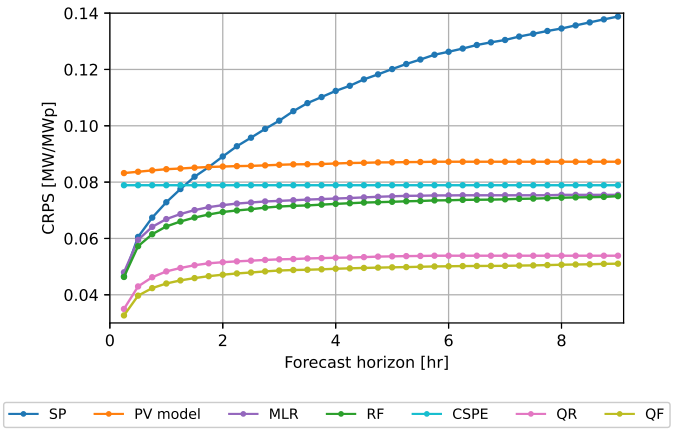

Fig. 4: The average CRPS of the ID single-value and probabilistic forecasting models per forecast horizon.

in case of perfect forecasting. Similarly, the imbalance caused almost halves (-46.3%).

Overall, the probabilistic models exhibit superior performance compared to the other models across the majority of time horizons in terms of generating the highest revenues and minimizing imbalances (see Table IV). Only SP demonstrates competitive results for $k = 1$ and $k = 4$. Among the considered horizons, QF produces the lowest imbalance, while QR achieves the highest revenues for most instances.

D. Trading revenues to forecast accuracy

Although from Table IV it appears that improved model accuracy's (lower imbalances) lead to higher revenues, closer inspection of the results show that the imbalance and revenues are not linearly related. Exemplary for this is the relative high imbalance caused by SP for $k = 4$, while it earns the highest revenues. This relation is further explored in Fig. 5, which explicitly plots the revenues to the CRPS. First focusing on Fig. 5b, it can observed that improved model accuracy does not lead to higher revenues. For example, the RF model obtains a significantly lower CRPS compared to MLR and SP, but yields lower market trading revenues. In short, this is explained by the state of the electricity system being either short or long at the time an imbalance occurs.

Yet, focusing on a specific model, e.g. MLR, it can be noticed that the generated revenues increase with improved accuracy, resulting from reduced forecast lead-times. This observation is supported by Fig. 5a, which indicates an approximate linear relation between the accuracy and economic revenue per forecast model; this trend is observed for MLR, RF, QR, QF or SP.

E. Imbalance penalty sensitivity analysis

Both a static and dynamic strategy are considered for setting the imbalance penalty as part of the stochastic bidding approach, see problem (1) and (3). Fig. 6 presents the results for these two strategies for $k = 1$, while considering the QR model. Very similar results are found for the other forecast horizons as well as the QF model. Fig. 6 clearly shows that

TABLE IV: Numerical results of market participation per forecast model for several forecast horizons (k). The results for ID trading combine DA trades with one-off ID trades at the specified time horizon. The results of $k = 6$ and $k = 9$ are similar to $k = 3$. The technical column presents the quantitative results of trading energy. The economic column shows the net monetary results of market participation. DA presents the results for all energy traded in the DAM, whereas ID is the absolute sum of trades in the IM. IMB presents the total imbalance caused, i.e. absolute sum of the surplus (S) and deficit (D).

Model	Technical [MWh/MWp] DA	ID	S	D	IMB	Economic [€/MWp] DA	ID	S	D	Total
Perfect forecasting (PF)										
PF	1051					27080				27080
Forecast horizon: 15 min										
SP	1024	571	**96**	-116	212	28236	-306	2177	-3197	26910
PV	978	201	209	-151	360	26645	-1096	3531	-5946	23134
MLR	1008	341	105	-102	207	27676	-501	2087	-3245	26018
RF	1014	324	101	-99	200	27677	-362	1753	-3141	25926
CSPE	1080	236	250	-273	523	30109	-1454	3227	-13562	18321
QR	871	438	99	-99	198	23623	3803	2409	-2768	**27068**
QF	950	344	100	**-97**	**197**	25423	2019	2184	-2841	26785
Forecast horizon: 1 hr										
SP	1024	577	148	-203	352	28236	949	3133	-6557	**25760**
PV	978	191	209	-157	366	26645	-906	3421	-6299	22861
MLR	1008	285	148	-149	297	27676	-687	2533	-5460	24063
RF	1014	265	141	-137	277	27677	-410	2098	-5461	23903
CSPE	1080	236	250	-273	523	30109	-1454	3227	-13562	18321
QR	871	390	148	-135	283	23623	3165	3071	-4727	25133
QF	950	302	**140**	**-129**	**267**	25423	1542	2645	-4679	24930
Forecast horizon: 2 hrs										
SP	1024	572	182	-268	450	28236	2142	2946	-9954	23370
PV	978	185	207	-163	370	26645	-671	3277	-6641	22610
MLR	1008	267	160	-150	310	27676	-820	2396	-6292	22961
RF	1014	242	154	-146	300	27677	-589	1981	-6262	22807
CSPE	1080	236	250	-273	523	30109	-1454	3227	-13562	18321
QR	871	373	162	-144	306	23623	2929	2909	-5632	**23829**
QF	950	280	**151**	**-135**	**286**	25423	1203	2504	-5302	23827
Forecast horizon: 3 hrs										
SP	1024	542	206	-311	520	28236	2963	2928	-12436	21691
PV	978	182	206	-166	372	26645	-547	3208	-6813	22493
MLR	1008	259	163	-153	316	27676	-833	2292	-6562	22574
RF	1014	236	159	-149	308	27677	-688	1986	-6519	22457
CSPE	1080	236	250	-273	523	30109	-1454	3227	-13562	18321
QR	871	367	165	-147	312	23623	2889	2860	-5831	**23541**
QF	950	274	**158**	**-138**	**296**	25423	1057	2571	-5694	23357
Forecast horizon: 12-36 hrs										
SP	1024		296	-278	574	28236		2097	-13250	17083
PV	978		232	-169	401	26645		1526	-7224	20946
MLR	1008		217	-193	410	27676		1109	-8213	20572
RF	1014		**203**	-185	388	27677		876	-8065	20487
CSPE	1080		276	-314	590	30109		2401	-14140	18370
QR	871		277	**-133**	410	23623		4258	-5591	22291
QF	950		216	-151	**367**	25423		3380	-6455	**22348**

adopting the dynamic strategy results in higher economic revenues. For this scenario, a higher economic revenue is obtained when $|\lambda^+| \approx |\lambda^-|$ i.e. the imbalance penalty in case of a surplus or deficit is in balance, which is the case when $|c_1|$ is approximately equal to $|c_2|$. The single most optimal value i.e. highest economic value is indicated by the red dot. This is also the imbalance scenario considered in the results presented in Sections IV-C and IV-D. The optimal value for the dynamic strategy is found for low values of $|c_1|$ and $|c_2|$, where the imbalance price is approximately equal to the spot market price.

When relying on the static imbalance scenario, the economic revenues are maximized when λ^+ is positive and λ^- exceeds a value of approximately 30 €/MWh.

V. Discussion

Very few studies examined the value of solar power forecasting, which can be effectively assessed by considering the economic error metrics proposed in this study. In an earlier study [36], the authors suggest a *monotome* mapping of the

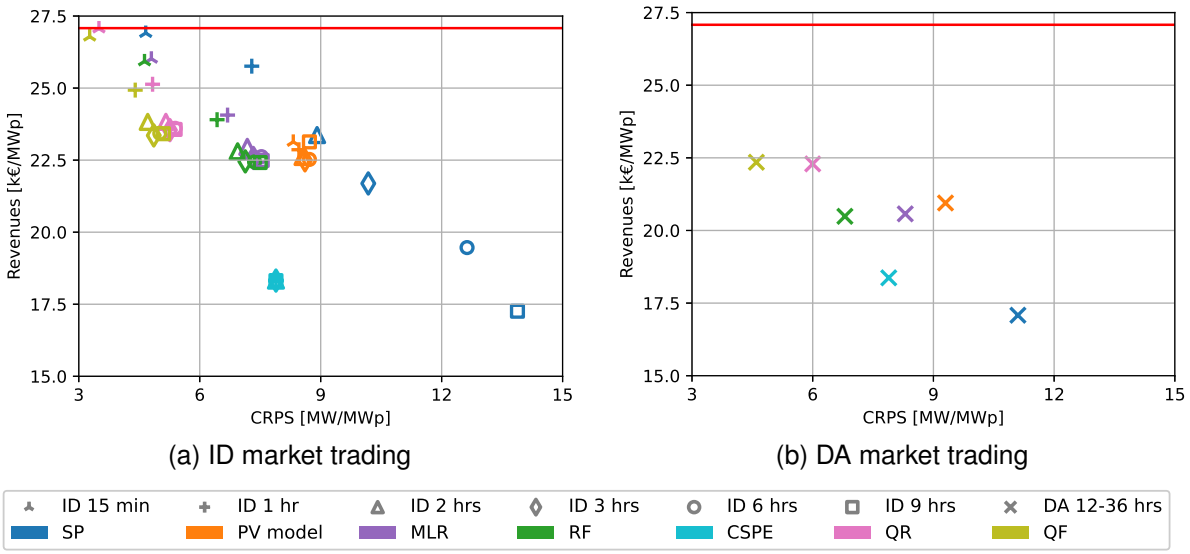

Fig. 5: The economic revenue as a function of the CRPS. The red line indicates the revenues in case of perfect forecasting.

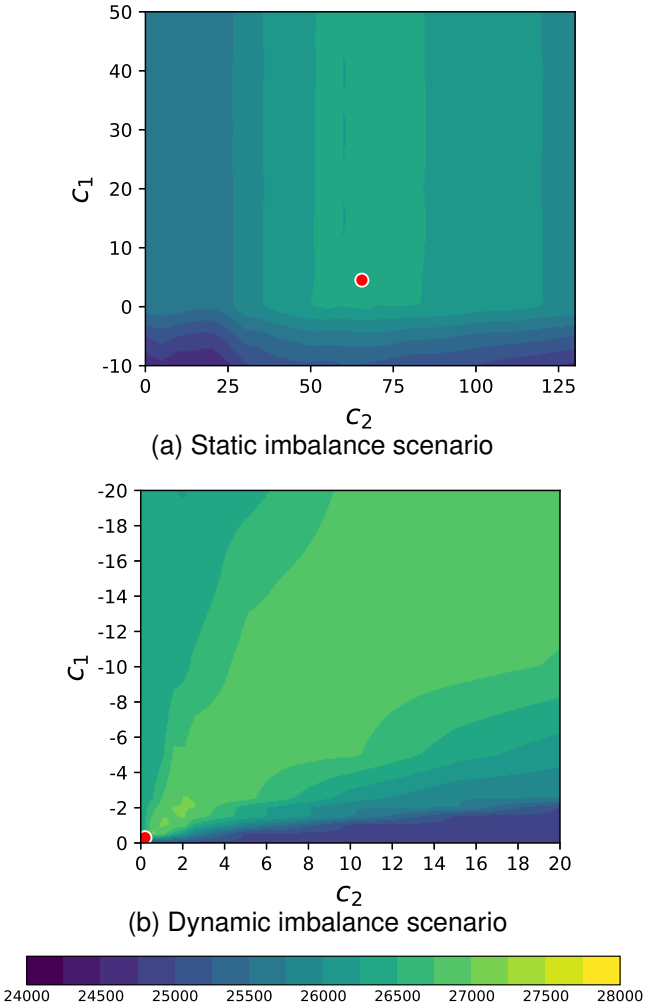

Fig. 6: Sensitivity analysis on the c_1 and c_2 value for the static and dynamic imbalance scenarios at $k = 1$. The color bar presents the obtained revenues in €/MWp, where the red dot indicates the optimal value.

quality and value, implying that a higher forecast quality corresponds to higher economic value. This is contradicted by the results presented in this study. Section IV-D shows that the economic value and accuracy are not linearly correlated. This is due to the dependence on the (real-time) market conditions, which was also discussed in [10]. Technical error metrics are therefore not sufficient to address the economic value of forecasts and this study identifies an added value of adopting economic metrics.

Firstly, economic metrics offer market participants that operate a PV plant valuable information on the most advantageous forecast model. The economic metric proposed in this study is capable of mapping the economic value of solar power forecasting modes by considering the market bidding process as well as the imbalance costs.

Secondly, the value of such economic metrics goes beyond market participants as the metrics provide insights into the ease of an electricity system to adequately manage the imbalance in real-time. The imbalance price is typically equal to the balancing energy price, which is set by the highest activated frequency restoration reserve bid on the merit order list. A higher imbalance price therefore corresponds to times where expensive assets are deployed to restore the system's balance and thus indicate periods where the system's imbalance is large and/or available balancing capacity is limited. On the other hand, low imbalance prices typically indicate periods where there is an abundance of electricity, available balancing capacity and/or the system's imbalance is limited. In this regard, evaluating a solar power forecasting model on its economic value and in particular considering the imbalance costs, gives an (indirect) indication of its effect on the electricity system.

Therefore, it is recommended to utilize metrics that assess the economic value of solar power forecasting models. This economic evaluation not only provides insights into the expected economic revenues but also offers an indication of an electricity system's capability to manage imbalances.

VI. Conclusion

This study proposes a novel multistage stochastic optimization model for market participants that operate a PV system. The method utilizes a statistical scenario generation method, which transforms probabilistic PV power forecasts into time-dependent scenarios. The results of this study show the effectiveness of the stochastic bidding approach. The method outperforms the reference method, as it obtains higher revenues and causes less imbalance. This study also shows the value of extending market participation from the DAM to IM, which is found to increase the revenues by 21%, while halving the total imbalance. Furthermore, the study explores the relation between the accuracy of solar power forecasting models and their value and demonstrates that these are not linearly related.

References

[1] I. PVPS, "Trends in photovoltaic applications 2023," Paris, Tech. Rep., 2023. [Online]. Available: https://iea-pvps.org/wp-content/uploads/2023/04/IEA_PVPS_Snapshot_2023.pdf

[2] O. Gandhi, D. S. Kumar, C. D. Rodríguez-Gallegos, and D. Srinivasan, "Review of power system impacts at high pv penetration part i: Factors limiting pv penetration," *Solar Energy*, vol. 210, pp. 181–201, 2020.

[3] C. Breyer, D. Bogdanov, A. Gulagi, A. Aghahosseini, L. S. Barbosa *et al.*, "On the role of solar photovoltaics in global energy transition scenarios," *Progress in Photovoltaics: Research and Applications*, vol. 25, no. 8, pp. 727–745, 2017.

[4] M. Q. Raza, M. Nadarajah, and C. Ekanayake, "On recent advances in pv output power forecast," *Solar Energy*, vol. 136, pp. 125–144, 2016.

[5] D. Yang, W. Wang, C. A. Gueymard, T. Hong, J. Kleissl *et al.*, "A review of solar forecasting, its dependence on atmospheric sciences and implications for grid integration: Towards carbon neutrality," *Renewable and Sustainable Energy Reviews*, vol. 161, p. 112348, 2022.

[6] T. Hong, P. Pinson, Y. Wang, R. Weron, D. Yang, and H. Zareipour, "Energy forecasting: A review and outlook," *IEEE Open Access Journal of Power and Energy*, vol. 7, pp. 376–388, 2020.

[7] P. Lauret, M. David, and P. Pinson, "Verification of solar irradiance probabilistic forecasts," *Solar Energy*, vol. 194, pp. 254–271, 2019.

[8] Y. Wang, D. Millstein, A. D. Mills, S. Jeong, and A. Ancell, "The cost of day-ahead solar forecasting errors in the united states," *Solar Energy*, vol. 231, pp. 846–856, 2022.

[9] J. Luoma, P. Mathiesen, and J. Kleissl, "Forecast value considering energy pricing in california," *Applied energy*, vol. 125, pp. 230–237, 2014.

[10] J. Antonanzas, D. Pozo-Vázquez, L. A. Fernandez-Jimenez, and F. Martinez-de Pison, "The value of day-ahead forecasting for photovoltaics in the spanish electricity market," *Solar Energy*, vol. 158, pp. 140–146, 2017.

[11] L. Visser, T. AlSkaif, and W. van Sark, "Operational day-ahead solar power forecasting for aggregated pv systems with a varying spatial distribution," *Renewable Energy*, vol. 183, pp. 267–282, 2022.

[12] A. Bracale, G. Carpinelli, P. De Falco, R. Rizzo, and A. Russo, "New advanced method and cost-based indices applied to probabilistic forecasting of photovoltaic generation," *Journal of Renewable and Sustainable Energy*, vol. 8, no. 2, p. 023505, 2016.

[13] P. Shinde, M. R. Hesamzadeh, P. Date, and D. W. Bunn, "Optimal dispatch in a balancing market with intermittent renewable generation," *IEEE Transactions on Power Systems*, vol. 36, no. 2, pp. 865–878, 2020.

[14] A. R. Silva, H. Pousinho, and A. Estanqueiro, "A multistage stochastic approach for the optimal bidding of variable renewable energy in the day-ahead, intraday and balancing markets," *Energy*, vol. 258, p. 124856, 2022.

[15] E. SPOT, "The European Power Exchange," 2022. [Online]. Available: https://www.epexspot.com/en

[16] A. V. Ntomaris, I. G. Marneris, P. N. Biskas, and A. G. Bakirtzis, "Optimal participation of res aggregators in electricity markets under main imbalance pricing schemes: Price taker and price maker approach," *Electric Power Systems Research*, vol. 206, p. 107786, 2022.

[17] R. A. Campos, G. L. Martins, and R. Rüther, "Assessing the influence of solar forecast accuracy on the revenue optimization of photovoltaic+ battery power plants in day-ahead energy markets," *Journal of Energy Storage*, vol. 48, p. 104093, 2022.

[18] A. Gonzalez-Garrido, A. Saez-de Ibarra, H. Gaztanaga, A. Milo, and P. Eguia, "Annual optimized bidding and operation strategy in energy and secondary reserve markets for solar plants with storage systems," *IEEE Transactions on Power Systems*, vol. 34, no. 6, pp. 5115–5124, 2018.

[19] F. Conte, S. Massucco, M. Saviozzi, and F. Silvestro, "A stochastic optimization method for planning and real-time control of integrated pv-storage systems: Design and experimental validation," *IEEE Transactions on Sustainable Energy*, vol. 9, no. 3, pp. 1188–1197, 2017.

[20] E. Perez, H. Beltran, N. Aparicio, and P. Rodriguez, "Predictive power control for pv plants with energy storage," *IEEE Transactions on Sustainable Energy*, vol. 4, no. 2, pp. 482–490, 2012.

[21] A. Saez-de Ibarra, V. I. Herrera, A. Milo, H. Gaztañaga, I. Etxeberria-Otadui, S. Bacha, and A. Padros, "Management strategy for market participation of photovoltaic power plants including storage systems," *IEEE Transactions on Industry Applications*, vol. 52, no. 5, pp. 4292–4303, 2016.

[22] T. Carriere, C. Vernay, S. Pitaval, F.-P. Neirac, and G. Kariniotakis, "Strategies for combined operation of pv/storage systems integrated into electricity markets," *IET Renewable Power Generation*, vol. 14, no. 1, pp. 71–79, 2020.

[23] M. David, J. Boland, L. Cirocco, P. Lauret, and C. Voyant, "Value of deterministic day-ahead forecasts of pv generation in pv+ storage operation for the australian electricity market," *Solar Energy*, vol. 224, pp. 672–684, 2021.

[24] L. Visser, T. AlSkaif, J. Hu, A. Louwen, and W. van Sark, "On the value of expert knowledge in estimation and forecasting of solar photovoltaic power generation," *Solar Energy*, vol. 251, pp. 86–105, 2023.

[25] P. Pinson, H. Madsen, H. A. Nielsen, G. Papaefthymiou, and B. Klöckl, "From probabilistic forecasts to statistical scenarios of short-term wind power production," *Wind Energy: An International Journal for Progress and Applications in Wind Power Conversion Technology*, vol. 12, no. 1, pp. 51–62, 2009.

[26] D. Van der Meer, G. C. Wang, and J. Munkhammar, "An alternative optimal strategy for stochastic model predictive control of a residential battery energy management system with solar photovoltaic," *Applied Energy*, vol. 283, p. 116289, 2021.

[27] D. Yang and D. van der Meer, "Post-processing in solar forecasting: Ten overarching thinking tools," *Renewable and Sustainable Energy Reviews*, vol. 140, p. 110735, 2021.

[28] J. Bröcker and L. A. Smith, "Increasing the reliability of reliability diagrams," *Weather and forecasting*, vol. 22, no. 3, pp. 651–661, 2007.

[29] T. L. Thorarinsdottir, M. Scheuerer, and C. Heinz, "Assessing the calibration of high-dimensional ensemble forecasts using rank histograms," *Journal of computational and graphical statistics*, vol. 25, no. 1, pp. 105–122, 2016.

[30] W. F. Holmgren, C. W. Hansen, and M. A. Mikofski, "pvlib python: A python package for modeling solar energy systems," *Journal of Open Source Software*, vol. 3, no. 29, p. 884, 2018.

[31] KNMI, "KNMI Data Platform," 2022. [Online]. Available: https://dataplatform.knmi.nl/dataset/cesar-surface-meteo-lc1-t10-v1-0

[32] ECMWF, "European Centre for Medium-range Weather Forecasts, ECMWF," 2020. [Online]. Available: https://www.ecmwf.int/en/forecasts/datasets/archive-datasets

[33] ENTSO-E, "European Network of Transmission System Operators for Electricity, ENTSO-E," 2020. [Online]. Available: https://transparency.entsoe.eu/

[34] A. Tijdink, M. Hoffman, R. Vrolijk, and B. Van Breukelen, "Annual Market Update 2021: Electricity market insights," TenneT, Tech. Rep., 2022. [Online]. Available: https://tennet-drupal.s3.eu-central-1.amazonaws.com/default/2022-07/Annual_Market_Update_2021_0.pdf

[35] TenneT, "Settlement prices," 2020. [Online]. Available: https://www.tennet.org/english/operational_management/export_data.aspx?exporttype=Onbalansprijs

[36] D. Yang, S. Alessandrini, J. Antonanzas, F. Antonanzas-Torres, V. Badescu, H. G. Beyer, R. Blaga *et al.*, "Verification of deterministic solar forecasts," *Solar Energy*, vol. 210, pp. 20–37, 2020.